

THE ACID-BASE PROPERTIES AND KINETICS OF DISSOLUTION OF THE  $\text{Fe}_4\text{S}_4$  CORES  
OF CHROMATIUM FERREDOXIN AND HIGH POTENTIAL IRON PROTEIN

Richard Maskiewicz, Thomas C. Bruice,\* and Robert G. Bartsch

Department of Chemistry, University of California at Santa Barbara, Santa Barbara, California 93106, and Department of Chemistry, University of California at San Diego, La Jolla, California 92037.

Received May 5, 1975

Summary

The kinetics for the dissolution of Chromatium ferredoxin and High Potential Iron Protein have been compared ( $\text{H}_2\text{O}$  = -1.05 to pH = 7). Chromatium ferredoxin hydrolyzes via a mechanism following the kinetics  $\text{A}^- + \text{H}^+ \rightleftharpoons \text{AH}^- \rightarrow \text{BH}^- \rightarrow \text{C}$  at constant pH. Initial absorbances describe a theoretical one proton titration curve corresponding to a  $\text{pK}_a$  of 2.7 for  $\text{AH}^-$ . Chromatium High Potential Iron Protein shows no titration behavior and hydrolyzes slowly in water. These results confirm the availability of the  $\text{Fe}_4\text{S}_4$ -cores of Chromatium ferredoxin as compared to that of High Potential Iron Protein. Further, these results establish similarities in the hydrolytic chemistry of protein bound  $\text{Fe}_4\text{S}_4$ -cores as compared to synthetic compounds of structure  $\text{Fe}_4\text{S}_4(\text{SR})_4^-$ .

Materials and Methods

Chromatium ferredoxin (C.Fd.) and Chromatium High Potential Iron Protein (HIPIP) were prepared by a published method (1). The ferredoxin had a purity index ( $A_{278}/A_{384}$ ) of 2.09, and HIPIP ( $A_{283}/A_{388}$ ) 2.56.

Rates and absorbances were obtained using a Durrum model D-110 stopped-flow spectrophotometer (under a  $\text{N}_2$  atmosphere) with a Biomation model 805 waveform recorder. Titration curves were obtained by plotting initial absorbances of the starting species of the observed biphasic hydrolysis reaction as a function of  $-\log$  (hydrogen ion activity) i.e.  $\text{H}_2\text{O}$  and pH. Initial absorbances were measured 3 msec after completion of stopped flow mixing. All rate processes were followed at 390 nm. Measurements were performed anaerobically under pseudo-first-order conditions ( $[\text{buffer}] > 100$  [iron-sulfur protein]) and at an ionic strength of 0.1 (KCl) at all pH's

greater than 1.0. HCl was employed as a buffer between  $H_0$  (-0.45) and pH 3.43. Formate was employed at pH 3.72, acetate at pH 4.63, and buffering was not required to hold the adjusted pH between pH 4.63 and 6.85.

### Results and Discussion

Initial absorbances of the iron-sulfur clusters in Chromatium ferredoxin obtained 3 msec after mixing protein and buffer solutions are shown as a function of pH in Figure 1. The points correspond to the theoretical curve of a simple one proton dissociation. The curve of Figure 1 represents the dissociation of an acid of  $pK_a$  2.72. Chromatium HIPIP initial absorbances, shown in the inset in Figure 1, evidence spectral change only below pH 1.0.

As shown in Figure 2, the hydrolytic reaction of the  $Fe_4S_4$  clusters in the ferredoxin showed biphasic behavior ( $AH^- \rightarrow BH^- \rightarrow C$ , where  $AH^-$  represents an initial protonated form of an active site cluster  $A^-$ , and C represents hydrolysis products). In order to determine the pH-dependence

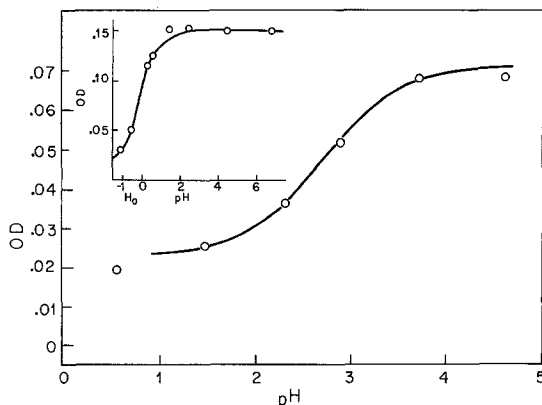


Figure 1. Spectrophotometric acid dissociation curve for the protonated  $Fe_4S_4$  clusters (i.e.,  $AH^-$ ) of Chromatium ferredoxin. The inset represents a spectrophotometric titration of Chromatium High Potential Iron Protein. All optical densities were measured 3 msec after completion of stopped-flow mixing.

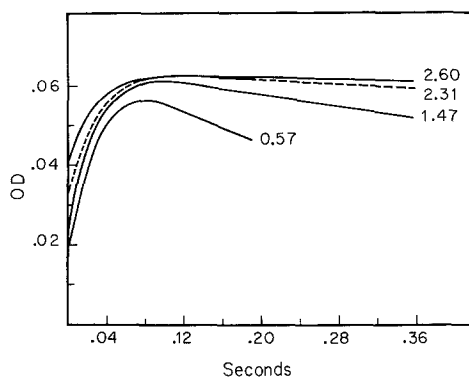


Figure 2. Optical density of Chromatium ferredoxin as a function of time at various pH's. The optical densities at  $t=\infty$  were zero at these pH's.

of the rate constants for  $AH^- \rightarrow BH^- \rightarrow C$  it was necessary to take into account: (1) the extinction coefficient of  $A^-$  exceeds  $AH^-$  ( $\epsilon_A/\epsilon_{AH^-} = 3.44$ ); (2) the absorbance of  $BH^-$  as well as the rate constant for conversion of  $AH^-$  to  $BH^-$  ( $k_{AH^- \rightarrow BH^-} = 29 \text{ sec}^{-1}$ ) are pH-independent; and (3) the conversion of  $BH^-$  to  $C$  exhibits the pH-dependence shown in Figure 3. In order to explain the pH-independence of the absorbance of  $BH^-$ , one may assume that the conversion of  $AH^- \rightarrow BH^-$  involves a slow conformational change with concomitant intramolecular proton transfer from the protonated  $Fe_4S_4$ -core of  $AH^-$  to surrounding protein resulting in the reformation of unprotonated  $Fe_4S_4$  cluster in  $BH^-$ . This assumption would be in accord with the observation that the absorbance of the species  $BH^-$  is similar to that of the native unprotonated protein (i.e.,  $A^-$ ). The line of Figure 3, which exhibits limiting slopes of -1, 0, and -2 with increasing pH, was generated from the empirical expression of equation 1

$$k_{\text{obs}} = \frac{V(a_H)^3 + W(a_H)^2}{X(a_H)^2 + Y(a_H) + Z} \quad (1)$$

previously employed to correlate the hydrogen ion concentration with the

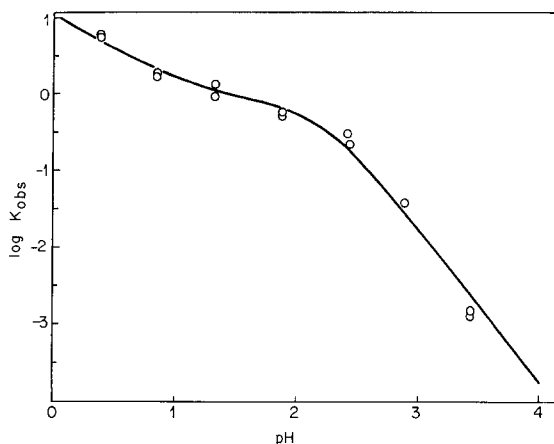
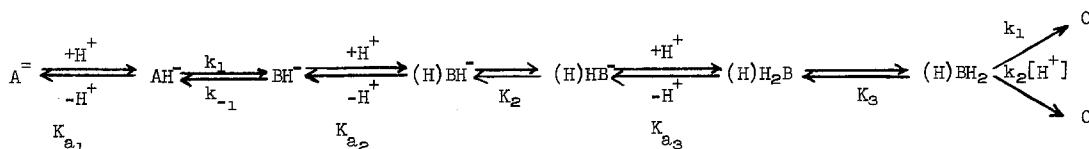


Figure 3. Log  $k_{\text{obs}}$  vs pH rate profile for the dissolution of the  $\text{Fe}_4\text{S}_4$  clusters in Chromatium ferredoxin. Reactions were carried out in  $\text{H}_2\text{O}$  at  $30^\circ$ ,  $\mu = 0.1$ . The points are experimental and the line was generated using equation 1 and the constants provided with Scheme I.

rate of hydrolysis of synthetic  $\text{Fe}_4\text{S}_4$  clusters (2). Native HIPIP hydrolyzed at approximately  $10^{-4}$  the rate of the ferredoxin in water, and approximately  $10^{-2}$  as fast in a 70/30 vol. percent DMSO/ $\text{H}_2\text{O}$  solution.

The pH-dependence of the overall hydrolysis reaction ( $\text{AH}^- \rightarrow \text{BH}^- \rightarrow \text{C}$ ) for C.Fd. may be explained via Scheme I. As in the case of the synthetic analogs previously studied by us, any hydrolysis mechanism for  $\text{BH}^- \rightarrow \text{C}$

Scheme I



$$K_{a_1} = \frac{[\text{A}^-][\text{H}^+]}{[\text{AH}^-]} = 1.90 \times 10^{-3}; \quad \frac{k_{-1}}{k_1} = \frac{[\text{AH}^-]}{[\text{BH}^-]}, \quad k_1 + k_{-1} = 29 \text{ sec}^{-1}; \quad K_{a_2} = \frac{[\text{BH}^-][\text{H}^+]}{[(\text{H})\text{BH}^-]} = 5 \times 10^2;$$

$$K_2 = \frac{[(\text{H})\text{BH}^-]}{[(\text{H})\text{HB}^-]} = 1 \times 10^{-2}; \quad K_{a_3} = \frac{[(\text{H})\text{HB}^-]}{[(\text{H})\text{H}_2\text{B}^-]} = 1 \times 10^1; \quad K_3 = \frac{[(\text{H})\text{H}_2\text{B}^-]}{[(\text{H})\text{BH}_2^-]} = 8 \times 10^{-7}; \quad k_1 = 7 \times 10^{-1};$$

$$k_2 = 1 \times 10^1$$

must recognize at least two proton dissociation equilibria and at least one acid catalyzed rate determining step. One of the two acid-base equilibria must pertain to the established preequilibrium protonation of the iron-sulfur cluster, and the other to that of an intermediate. An additional restraint is that any mechanistic scheme which is devised must not directly reflect the true  $pK_a$  in the derived  $\log k_{\text{obs}}$  vs pH profile. Scheme I satisfies these criteria and provides for the derivation of equation (2). Since  $k_{\text{AH}^- \rightarrow \text{BH}^-}$  is large compared to  $k_{\text{BH}^- \rightarrow \text{C}}$  at all pH's,

$$k_{\text{obs}} = \frac{(k_1 + k_2 a_{\text{H}}) a_{\text{H}}^3}{(K_3 + 1) a_{\text{H}}^3 + K_3 K_{a_3} (K_2 + 1) a_{\text{H}}^2 + K_2 K_3 K_{a_2} K_{a_3} \left( \frac{k_{-1}}{k_1} + 1 \right) a_{\text{H}} + \frac{k_{-1}}{k_1} K_2 K_3 K_{a_1} K_{a_2} K_{a_3}} \quad ($$

equation (2) can be reduced to equation (3). This is of the same form as

$$k_{\text{obs}} = \frac{k_1 + k_2 a_{\text{H}}) a_{\text{H}}^2}{(K_3 + 1) a_{\text{H}}^2 + K_3 K_{a_3} (K_2 + 1) a_{\text{H}} + K_2 K_3 K_{a_2} K_{a_3}} \quad ($$

empirical equation (1) employed to fit the profile of Figure 3. Scheme I entails initial protonation of one or both of the  $\text{Fe}_4\text{S}_4$  clusters to give the species  $\text{AH}^-$  (for which the titration curve of Figure 1 was obtained). The species  $\text{AH}^-$  is converted via a conformational change to  $\text{BH}^-$  in a reaction which is otherwise pH-independent. A subsequent equilibrium protonation results in the conversion of  $\text{BH}^-$  to a more hydrolytically labile species  $(\text{H})\text{BH}^-$ . The species  $(\text{H})\text{BH}^-$  is then converted to  $(\text{H})\text{HB}^-$  in an equilibrium reaction which involves the formation of an -SH moiety. Species  $(\text{H})\text{HB}^-$  then undergoes an equilibrium protonation to yield  $(\text{H})\text{H}_2\text{B}$  which proceeds in an equilibrium reaction to  $(\text{H})\text{BH}_2$  with formation of an additional -SH moiety. The rate determining steps in the hydrolysis of the cluster involves spontaneous ( $k_1$ ) and specific acid catalyzed ( $k_2[\text{H}^+]$ ) reactions of  $(\text{H})\text{BH}_2$ . A detailed discussion of the mechanism will be provided elsewhere. The constants provided in Scheme I were obtained in the following manner. The constant  $K_{a_1}$  was obtained from the titration curve of Figure 1 and  $k_1 + k_{-1}$

were obtained as a sum expressed as  $k_{AH^- \rightarrow BH^-}$  which was employed in the fit of the  $AH^- \rightarrow BH^- \rightarrow C$  kinetics of the overall hydrolysis reaction as shown in Figure 2. The remaining constants were obtained as values which provide a line fitting the experimental points of Figure 3 employing equation (3).

The present investigation establishes that protein bound  $Fe_4S_4$  clusters possess acid dissociation constants as do their synthetic analogs. Thus, a  $pK_a$  of 2.72 for C.Fd. may be compared with one of 3.92 determined for the alkyl substituted analog,  $[Fe_4S_4(SCH_2CH(CH_3)_2)_4]^{2-}$  (solv. 60/40 vol. percent N-methylpyrrolidinone/ $H_2O$ ) (2). The observation of a single titration curve for C.Fd., which contains two  $Fe_4S_4$  clusters, implies either very similar cluster environments or the unavailability of one of the clusters. The first case is preferred since both clusters are rapidly hydrolyzed. The unavailability of the  $Fe_4S_4$  cluster of HIPIP for either protonation (over the pH range 0 to 7), or hydrolysis relative to that of C.Fd., is in accord with the established inaccessibility of the iron-sulfur cluster in native HIPIP toward reducing agents in water and with x-ray crystallographic indication of a protective peptide sheath surrounding the  $Fe_4-S_4$  cluster (3). As in the case of reduction of HIPIP (4), its hydrolysis is accelerated on transfer from water to DMSO/ $H_2O$ . This is presumably due to a conformational change.

#### ACKNOWLEDGEMENT

This work was supported by a grant to T.C.B. from the National Institutes of Health.

#### References

1. Bartsch, R. G. (1971) in *Methods in Enzymology*, Vol. XXII, Part A, A. San Pietro, ed., pp. 644-649, Academic Press, New York.
2. Bruice, T. C., Maskiewicz, R., and Job, R. (1975) *Proc. Natl. Acad. Sci. USA*, 72, 231-234.
3. Carter, C. W. Jr., Kraut, J., Freer, S. T., Xuong, N., Alden, R. A., and Bartsch, R. G. (1974) *J. Biol. Chem.*, 249, 4212-4225.
4. Cammack, R. (1973) *Biochem. Biophys. Res. Commun.*, 54, 548-554.